JOURNAL OF SOLID STATE CHEMISTRY **130,** 277–283 (1997)
ARTICLE NO. SC977327

Synthesis and Characterization of a Metastable $LnTh_2F_{11}$ Series (Ln = La–Lu, Y) with Cationic and Anionic Disorder: Crystal Structure of $SmTh_2F_{11}$

A. Abaouz,* A. Taoudi,† and J. P. Laval†,[1]

*Université Moulay Ismaïl, Faculté des Sciences, Meknès, Morocco; and †Laboratoire de Matériaux Céramiques et Traitements de Surface, URA–CNRS No. 320, Université de Limoges, 123, Avenue A. Thomas, 87060 Limoges Cedex, France

Received October 30, 1995; in revised form January 6, 1997; accepted February 4, 1997

A series of apparently stoichiometric and metastable phases of composition $LnTh_2F_{11}$ (Ln = La–Lu) was prepared for the first time. The crystal structure of $SmTh_2F_{11}$ was determined from single-crystal data with direct methods and refined to $R_1 = 0.043$ and $wR_2 = 0.107$ [space group: *Pnma*; $a = 861.0(2)$ pm, $b = 413.7(1)$ pm, $c = 722.5(2)$ pm; $Z = 1.33$]. This new structure type is characterized by a (Th + Sm) disorder on the 4*c* cationic site and by the presence of anionic vacancies on three of the four 4*c* anionic sites. The ideal MF_4 structure is a three-dimensional network of interconnected MF_{11} polyhedra but the coordination number of the cations is locally reduced to eight for Sm^{3+}. The structural relationship with the LaF_3 (tysonite) type is discussed.

INTRODUCTION

The systems of lanthanoid fluorides and tetravalent cations are the subject of numerous studies. Nonstoichiometric phases $(Ln, Zr)(O, F)_{3+x}$ (1–3) with structures derived from ReO_3-type by anion excess, homologous to phases $(M, Zr)(O, F)_{3+x}$ with M = Ca, Mg, transition metals (3), are described. Various degrees of cationic ordering are observed in these phases, depending on the size or the charge of the Ln, M cations, and on the annealing temperature. The excess of anions is accommodated by a statistical substitution of some X corners in MX_6 octahedra by X–X edges, the cationic coordination so increasing from 6 to 7 or 8. The "anion-excess ReO_3-type" can be described as a three-dimensional framework of corner-sharing MX_6 octahedra, MX_7 pentagonal bipyramids, and MX_8 dodecahedra. The homogeneity domain and the stability of the cubic $Pm\bar{3}m$ solid solutions are generally less extended with Ln^{3+} cations than with transition metals (3), and these metastable phases are more stable for the smallest Ln^{3+} cations. Several kinds of ternary fluorides involving a higher level of ordering are known.

– monoclinic $SmZrF_7$-type phases (4, 5), stable for all Ln cations and for Y;

– orthorhombic $PrZr_2F_{11}$-type compounds (6), strictly stoichiometric and stable only for Ln = La, Ce, Pr, and Nd and also for Hf^{4+} (7);

– rhombohedral ($R3m$ space group) β-$PrZr_3F_{15}$-type compounds (8), stoichiometric and obtained only for Ln = Pr and Nd at low temperature ($T < 800$°C).

Besides the previous fluorides, rhombohedral ($R\bar{3}c$ space group) α-MZr_3F_{15} phases constitute the most extended group, isolated for all rare earths (9–11) and also for M = Bi (12), In (13), U^{III} (14), Ti^{III} (13), and Tl^{III} (15). Homologous MM'_3F_{15} phases are known for M' = Hf with M = Sc (16) or Ln = Pr, Sm–Lu (10) and also for $M' = Tb^{IV}$ with M = Sc or $Ln = Tb^{III}$–Lu (17). The structure of $BiZr_3F_{15}$ is described (12) and more recently the structural comparison of a α-MZr_3F_{15} series with M cations of decreasing size: Pr, Eu, Gd, Y, Yb, Lu, Tl, and In showed a progressive change of the cation distribution of sixfold and eightfold sites between Zr and the smallest trivalent cations Lu, Tl, and In (11). A relationship of this structure type with the β-$PrZr_3F_{15}$ type was established.

Until now, no crystalline phases had been reported in binary systems LnF_3–ThF_4 in spite of the great deal of studies involving lanthanoid–thorium fluoride glasses, except a short note about the existence of a phase $CeTh_2F_{11}$ of limited stability (18) and a structural study of a hydrated phase $LaTh_4F_{19}.H_2O$ (19). Therefore, it was decided to investigate these systems using synthesis in sealed tubes which favor the quenching of metastable phases that are perhaps present, as in homologous LnF_3–ZrF_4 systems.

SYNTHESIS AND PRELIMINARY CHARACTERIZATION

$LnTh_2F_{11}$ phases were synthesized by direct reaction of the suitable mixture of lanthanoid fluoride and thorium

[1] To whom correspondence should be addressed.

0022-4596/97 $25.00

fluoride. The starting fluorides had been prepared by dehydration under anhydrous HF flow of the corresponding hydrated fluorides obtained by dissolution of the oxides in 40% HF solution. The mixtures were heated for one day at 950° in sealed nickel or platinum tubes and then quenched in water. For Ln = Nd–Dy, the new phases are generally obtained in a pure form but those corresponding to the lightest and the heaviest lanthanoids (La–Pr and Ho–Lu(Y)) are much more difficult to prepare and generally contain significant amounts of unreacted ThF_4 and LnF_3, indicating the metastable character of these phases. The X-ray diffraction pattern of the $LnTh_2F_{11}$ pure phases does not change with composition and traces of ThF_4 or LnF_3 phases immediately appear already near to the nominal composition, demonstrating the absence of other phases in the binary systems under our synthesis conditions. After annealings at different temperatures below 850°C, the X-ray patterns systematically show the presence of only ThF_4 and LnF_3 phases. The phases obtained in an impure form also seem to be strictly stoichiometric and their cell parameters do not vary with composition.

Small platelets corresponding to $SmTh_2F_{11}$ phase were obtained after a 3-day-heating at 950°C of a stoichiometric mixture of SmF_3–$2ThF_4$, and one of these crystals was selected for the crystallographic study. The space group, *Pnma* or $Pna2_1$, and the unit cell parameters were determined from the X-ray diffraction pattern recorded on a P4 Siemens four-circle diffractometer using Mo$K\alpha$ radiation and a graphite monochromator. The cell parameters of the isotypic $LnTh_2F_{11}$ series were refined from powder samples recorded on a Siemens D5000 diffractometer equipped with

TABLE 1
Cell Parameters of $LnTh_2F_{11}$

	a (pm)	*b* (pm)	*c* (pm)
La	870.3(2)	417.7(1)	726.4(2)
Ce	868.5(2)	416.9(1)	725.7(2)
Pr	866.6(2)	416.1(1)	724.9(2)
Nd	864.7(2)	415.3(1)	724.1(2)
Sm	861.0(2)	413.7(1)	722.5(2)
Eu	858.8(2)	412.9(1)	721.7(2)
Gd	856.5(2)	412.1(1)	721.0(2)
Tb	854.3(2)	411.3(1)	720.2(2)
Dy	853.6(2)	410.5(1)	719.4(2)
Ho	851.7(2)	409.7(1)	718.6(2)
Y	849.8(2)	408.9(1)	717.8(2)
Er	848.0(2)	408.1(1)	717.0(2)
Tm	846.1(2)	407.3(1)	716.3(2)
Yb	844.3(2)	406.5(1)	715.5(2)
Lu	842.4(2)	405.7(1)	714.7(2)

TABLE 2
X-ray Powder Diffraction Pattern of $TbTh_2F_{11}$

h	*k*	*l*	d_{exp} (pm)	d_{cal} (pm)	I/I_0	*h*	*k*	*l*	d_{exp} (pm)	d_{cal} (pm)	I/I_0
1	0	1	550.7	550.6	14	1	0	4	176.18	176.17	5
2	0	0	427.1	427.2	37	1	2	2	174.78	174.80	9
2	0	1	367.5	367.4	45	4	1	2	167.74	167.73	5
0	1	1	357.2	357.2	100	5	0	1	166.27	166.25	3
1	0	2	331.9	331.8	44	2	0	4	165.91	165.91	3
1	1	1	329.5	329.5	38	2	2	2	164.89	164.76	9
2	1	0	296.3	296.3	17	3	2	1	162.43	162.43	9
2	0	2	275.4	275.3	5	1	1	4	161.96	161.94	2
2	1	1	274.0	274.0	11	5	0	2	154.36	154.37	2
3	0	1	264.9	264.8	7	5	1	1	154.16	154.13	3
1	1	2	258.2	258.3	5	2	1	4	153.87	153.86	5
1	0	3	231.1	231.1	3	1	2	3	153.64	153.63	3
2	1	2	228.8	228.8	3	4	2	1	145.12	145.10	9
2	0	3	209.26	209.27	2	5	1	2	144.53	144.52	8
0	1	3	205.67	205.66	2	3	1	4	142.75	142.72	4
4	0	1	204.74	204.76	19	6	0	0	142.38	142.39	4
1	1	3	201.49	201.48	25	6	0	1	139.68	139.68	4
3	1	2	196.30	196.29	35	5	0	3	139.21	139.20	4
1	2	1	192.68	192.66	3	3	2	3	136.92	136.94	8
4	1	0	189.56	189.55	10	0	1	5	135.94	135.94	5
2	1	3	186.53	186.52	2	0	3	1	134.68	134.68	4
2	2	0	185.32	185.30	5	1	2	4	133.80	133.79	3
3	0	3	183.52	183.54	14	1	3	1	133.06	133.04	3
0	0	4	180.02	180.04	3	6	1	1	132.25	132.26	13
2	2	1	179.44	179.45	9	5	1	3	131.87	131.86	8
0	2	2	178.59	178.58	3						

a back-monochromator (Cu$K\alpha$ radiation). These parameters are reported in Table 1, and the indexed powder pattern of $TbTh_2F_{11}$ is given in Table 2.

CRYSTAL STRUCTURE OF $SmTh_2F_{11}$

Structure Determination

The X-ray diffraction intensities of the $SmTh_2F_{11}$ platelet were collected on the same four-circle diffractometer under the experimental conditions reported in Table 3.

The direct methods using Shelxs86 (20) allowed to localize one cation site in 4*c* (*Pnma* space group). After refinement of this position with Shelxl93 (20), the anions were located on four 4*c* sites after a Fourier-difference calculation and then refined. No other cationic site being detected, it was concluded that a complete cationic disorder is present in the structure. After refinement of the atomic coordinates and the anisotropic thermal vibration coefficients for all sites, the site occupancy of the cationic and anionic sites was allowed to vary. The refined cationic distribution closely corresponds to the experimental value and it has then been set to the 1 : 2 ratio. The $F(1)$, $F(2)$, and $F(4)$ anionic sites are clearly only partly filled (Table 4). The refined structural formula, $Sm_{1.33}Th_{2.67}F_{13.76}$ is reasonably close to the theoretical value: $Sm_{1.33}Th_{2.67}F_{14.67}$, considering on the one hand the limited accuracy of fluoride occupancies refined in the presence of heavy Th and Sm cations and on the other hand the uncertainties resulting from the cationic disorder. A reduction of Sm^{3+} to Sm^{2+} is ruled out because of the steady variation of the cell parameters in the $LnTh_2F_{11}$ series (Table 1). The presence of other weakly occupied anionic sites corresponding to the hypothetic formation of anionic clusters could not be detected on Fourier-difference maps and the structure was finally refined to $R_1 = 0.046$ and $wR_2 = 0.107$ for all data (0.043 and 0.104 for $I > 2\sigma(I)$) after introduction of anisotropic thermal factors, of an extinction coefficient and of a weighting scheme. Some small residues of electronic density (3000 e nm^{-3}) remain, reflecting the difficulty to perfectly refine such a statistical structure. However, all thermal vibration factors, especially anionic ones, have high but rather normal values, in accordance with the closeness of Th^{4+} and Sm^{3+} ionic radii (respectively, 113.4 and 109 pm in ninefold coordination). Calculations in the noncentrosymmetric $Pna2_1$ space group do not allow any improvement of the refinement.

The refined atomic coordinates are reported in Table 4, the main interatomic distances in Table 5 and the anisotropic displacement parameters in Table 6.

TABLE 3
Crystal Data and Structure Refinement for $SmTh_2F_{11}$

Empirical formula	$Sm_{0.33}Th_{0.667}F_{3.667}$
Wavelength	Mo$K\alpha$ (71.073 pm)
Crystal system	orthorhombic
Space group	*Pnma*
Unit cell dimensions	$a = 861.0(2)$ pm $b = 413.7(1)$ pm $c = 722.5(2)$ pm
Volume	$257.35(11).10^6$ pm^3
Z	4
Density (exp.)	7.00 Mg/m^3
Density (calc.)	7.08 Mg/m^3
Absorption coefficient	45.9 mm^{-1}
$F(000)$	421
Crystal size	$0.12 \times 0.12 \times 0.02$ mm
Theta range for data collection	3.68 to 30.07°
Index ranges	$-12 \le h \le 12$, $-5 \le k \le 5$, $-10 \le l \le 10$
Reflections collected	852
Independent reflections	426 [R(int) = 0.0579]
Refinement method	Full-matrix least-squares on F^2
Data/restraints/parameters	426/0/35
Goodness-of-fit on F^2	1.12
Final R indices [$I > 2\sigma(I)$]	$R_1 = 0.043$, $wR_2 = 0.104$
R indices (all data)	$R_1 = 0.046$, $wR_2 = 0.107$
Extinction coefficient	0.0040(14)
Largest diff. peak and hole	3000 and -3200 e nm^{-3}

TABLE 4
Atomic Coordinates ($\times 10^4$) and Equivalent Isotropic Displacement Parameters (pm$^2 \times 10^{-1}$) for $SmTh_2F_{11}$. $U_{eq.}$ is Defined as One Third of the Trace of the Orthogonalized U_{ij} Tensor

Atom	x	y	z	$U_{eq.}$	Occupancy[a]
Th	8225(1)	2500	3438(1)	0.017(1)	0.333
Sm	8225(1)	2500	3438(1)	0.017(1)	0.167
F(1)	2898(22)	2500	4904(25)	0.050(6)	0.43(3)
F(2)	2159(26)	2500	8333(19)	0.038(6)	0.39(3)
F(3)	578(13)	2500	1935(14)	0.025(2)	0.50(3)
F(4)	135(17)	2500	5818(20)	0.035(5)	0.40(2)

[a] The occupancy factor is set to 0.50 for a fully occupied special position 4*c* $(x, 1/4, z)$ of the *Pnma* space group.

TABLE 5
Selected Bond Lengths (pm) for $SmTh_2F_{11}$

Sm, Th–F(3)		229.5(11)
Sm, Th–F(3)^2		229.9(11)
Sm, Th–F(4)^2		237.9(14)
Sm, Th–F(1)^2		243.0(2)
Sm, Th–F(2)	2×	245.5(7)
Sm, Th–F(2)^2		250.7(14)
Sm, Th–F(4)	2×	256.2(8)
Sm, Th–F(1)	2×	257.9(11)
Sm, Th–Sm, Th		413.7(1) face-sharing
Sm, Th–Sm, Th		434.6(1) edge-sharing
Sm, Th–Sm, Th		451.3(1) corner-sharing

TABLE 6

Anisotropic Displacement Parameters ($pm^2 \times 10^{-1}$) for $SmTh_2F_{11}$. The Anisotropic Displacement Factor Exponent Takes the Form: $-2\pi^2[h^2a^{*2}U_{11} + \cdots + 2hka^*b^*U_{12}]$

	U_{11}	U_{22}	U_{33}	U_{23}	U_{13}	U_{12}
Th, Sm	6(1)	25(1)	21(1)	0	0(1)	0
F(1)	30(10)	58(10)	62(12)	0	−7(7)	0
F(2)	31(11)	51(10)	33(9)	0	−5(6)	0
F(3)	10(5)	41(5)	23(4)	0	7(3)	0
F(4)	22(8)	50(9)	33(8)	0	−6(6)	0

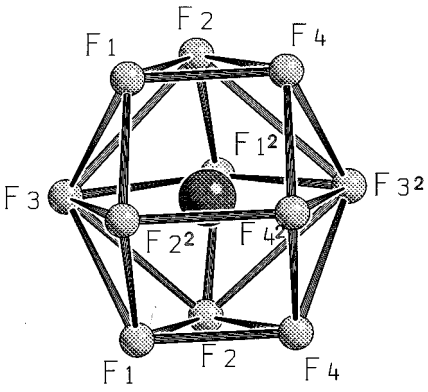

FIG. 2. (Sm, Th)F_{11} polyhedron.

Description of the Structure and Discussion

Figure 1 shows a projection of the $SmTh_2F_{11}$ structure onto the *xz* plane and Fig. 2 represents the coordination polyhedron about the mixed Sm–Th cation. This cation is surrounded, leaving out the incomplete occupancy of three anionic sites, by eleven anions (2 *F*(3) at short distance: 229.5 and 229.9 pm, 3 F(1), 3 F(2), and 3 F(4) at longer distances ranging from 237.9 to 257.9 pm. The 3–5–3 (Sm, Th)F_{11} polyhedron (with the formalism of Ref. (19)) is similar to the LaF_{11} polyhedron in the tysonite structure of LaF_3 (Edshammar polyhedron) but more regular. It can be conveniently described as a distorted 1–5–1 pentagonal bipyramid, with the pentagonal basis at the same *y* coordinate as the cation and with the apices replaced by distorted F(1)–F(2)–F(4) triangular faces, parallel to the pentagonal basis.

The (Sm, Th)F_{11} polyhedra are stacked in chains by sharing these F(1)–F(2)–F(4) triangular faces along the *y* axis. Adjacent chains are connected by F(3) corners and form corrugated sheets perpendicular to the *z* axis (Fig. 3). Two successive sheets along *z* are shifted from *y*/2 and connected by F(4)–F(4) edges, as shown in Fig. 4, forming in this way a three-dimensional network of corner-, edge-, and face-sharing (Sm, Th)F_{11} polyhedra whose projection onto the *xz* plane is represented in Fig. 1.

In the structure, all cations and anions are located in identical *xz* planar sheets at $y = 0.25$ and 0.75. The anionic plane net (which can be called $[5^2.3^2]^2.[5^3.3]^2$ in Schlaffli notation) in one of these sheets is shown in Fig. 5. The cations of this sheet (at $y = 0.25$) and the projection onto this plane net of the cations of the sheet at $y = 0.75$ (drawn as dotted circles in the same figure) form a semiregular $3^2.4.3.4$ plane net (represented with dotted lines). This kind of net was thoroughly investigated by O'Keeffe and Hyde (21) who considered it as intermediate between regular 4^4 (square) and 3^6 (triangular) nets.

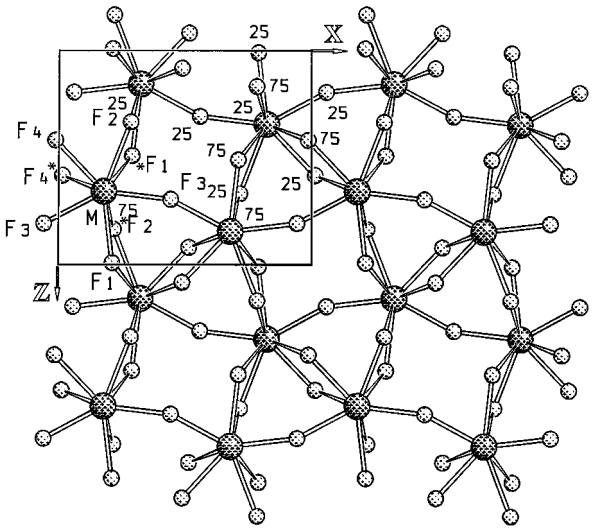

FIG. 1. Projection of the structure of $SmTh_2F_{11}$ onto the *xz* plane. For clarity, only the atoms between $y = 0$ and 1 are shown. Eight anions about every *M*(Sm, Th) cation are drawn. The three others form a second triangular F(1)*–F(2)*–F(4)* face exactly superposed to the first one.

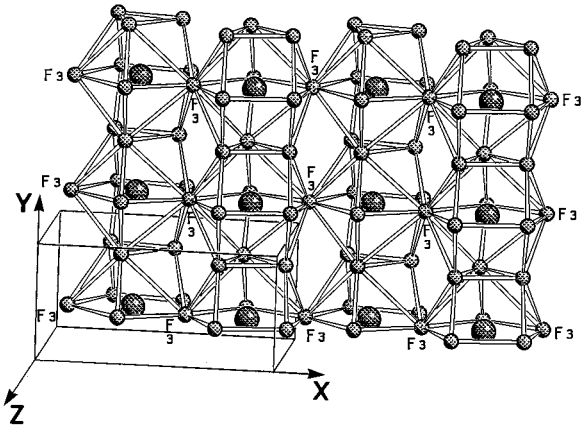

FIG. 3. Corrugated sheet formed from parallel columns of (Sm, Th)F_{11} polyhedra connected by F(3) corners, perpendicularly to the *z* axis.

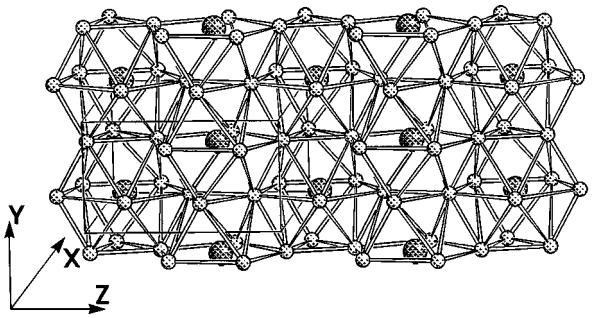

FIG. 4. Sheet formed from columns of $(Sm, Th)F_{11}$ polyhedra perpendicular to the x axis, showing the $y/2$ shift between successive edge-shared columns.

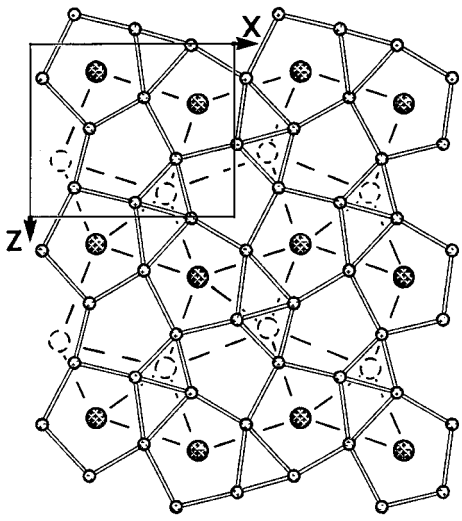

FIG. 5. Anionic $[5^2.3^2]^2.[5^3.3]^2$ plane net at $y = 0.25$. The cations at $y = -0.25$ are represented by dotted lines and cap triangular anionic faces at $y = 0.25$. With the cations at $y = 0.25$, their projection forms a $3^2.4.3.4$ semiregular net.

Comparison with tysonite structure. $SmTh_2F_{11}$ and LaF_3 (tysonite) structures can be related via a topological transformation from the $3^2.4.3.4$ plane nets previously described to 3^6 plane nets by puckering up of the lines of corner-shared MF_{11} polyhedra along the x direction. This puckering transforms the corner-sharing between adjacent MF_{11} columns (by F(3) corners) in edge-sharing and the anion-deficient MX_4 structure of $SmTh_2F_{11}$ to a slightly idealized MX_3 tysonite structure. Figure 6b represents the tysonite (almost) plane net homologue to the xz plane of $SmTh_2F_{11}$ in Fig. 6a. The other connections between MF_{11} polyhedra are very similar in both structures as attested by comparison of Fig. 7 with Fig. 4, though the $(Sm, Th)F_{11}$ polyhedron is more regular, as mentioned above. Thus, both structures are mainly correlated by the transformation : corner-sharing $\leftrightarrow$ edge-sharing, corresponding to the $MX_4 \leftrightarrow MX_3$ variation of composition. The structure of $SmTh_2F_{11}$ is therefore more open than the compact array characteristics of the tysonite structure.

Anion deficiency. The so far structure description considered an ideal MF_4 structure. In fact, only the F(3) site is completely filled, while the three other anionic sites have occupancies of 78–86%. If anionic vacancies were regularly distributed about each cation, the cationic coordination

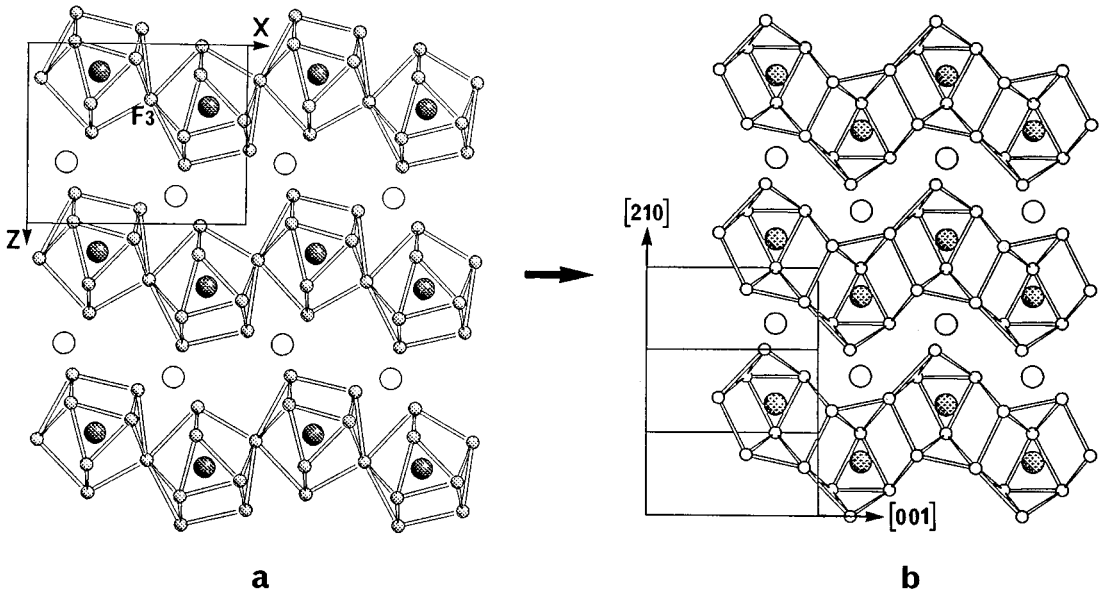

FIG. 6. Structural relationship between (a): $SmTh_2F_{11}$ and (b): LaF_3.

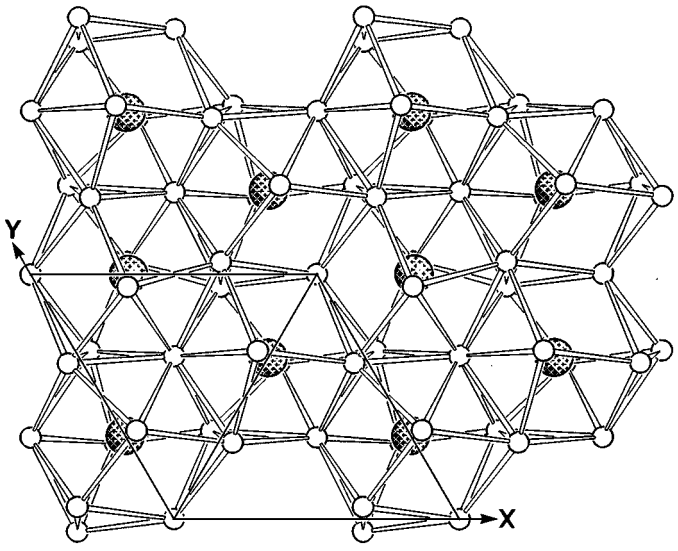

FIG. 7. Hexagonal stacking of LaF_{11} polyhedra, giving rise to linear columns similar to the $(Sm, Th)F_{11}$ analogues at Figs. 3 and 4.

would decrease from 11 to 10. However, the difference of charge between Sm^{3+} and Th^{4+} suggests the presence of a greater number of anionic vacancies about Sm^{3+}: indeed, if all of the vacancies are concentrated about the trivalent cation, its coordination becomes 8 which corresponds to a very similar coordination number/charge ratio for Sm^{3+} (2.67) and Th^{4+} (2.75) and hence to a good charge balance, because the ionic radii are also comparable. A low-coordination number for Ln^{3+} in the $LnTh_2F_{11}$ series could explain why this structure type exists for all rare-earth cations and especially for Yb^{3+} and Lu^{3+} which usually prefer a sevenfold or eightfold coordination. The greater stability of the series for Ln = Nd–Dy can be explained by the conjunction of two stabilizing factors:

– the closeness of the ionic radii of Th^{4+} and of the *Ln* cations of medium size,

– the great stability of eightfold coordination for the same *Ln* cations.

For larger size *Ln* cations, a progressive change in the distribution of anionic vacancies cannot be excluded.

Whatever the exact *Ln* coordination is, the absence of extra anion sites on Fourier-difference maps and the medium value of the anisotropic displacement parameters likely exclude an extensive clustering of anionic vacancies and a high cationic or anionic relaxation about these vacancies, as, e.g., in anion-excess fluorite structures. The defect structure probably corresponds to local transformations of some edge- and face-sharing connections between adjacent *Ln* polyhedra to corner-sharing ones. Therefore, such a process supposes a short range order between *Ln* and Th cations that the present study cannot determine more precisely. Further experiments involving neutron diffuse scattering on single crystals of high size should be necessary.

A long-range ordering of *Ln* and Th polyhedra was not observed even after long-time annealings, and hence an ordered $LnTh_2F_{11}$ variety is likely to be unstable.

CONCLUSION

The $LnTh_2F_{11}$ series presents interesting features. It constitutes a new anion-deficient MX_4 structure type, based on the stacking of the unusual MF_{11} polyhedra sharing triangular faces, edges and corners. This structure is less compact than LaF_3 tysonite type, one of the few structures built from MF_{11} polyhedra, and a simple relationship between both types is described. The metastability of the MTh_2F_{11} series is likely correlated with the cation disorder and with the presence of vacancies on 3 anionic sites. These vacancies are presumably localized about *Ln* cations whose coordination number so decreases from 11 to 8. These last structural features allow to compare this series, in spite of its different cationic framework, to nonstoichiometric phases derived from cubic ReO_3 type, e.g., $(Zr, Ln)(F, O)_{3+x}$, containing a disordered mixture of MX_6, MX_7, MX_8, and/or MX_9 polyhedra. The atomic distribution in the apparently stoichiometric $LnTh_2F_{11}$ series is intermediate between a complete anionic and cationic disorder, as described in cubic ReO_{3+x} phases, and the partial cationic disorder on two sites recently observed in a α-MZr_3F_{15} series (11). The great diversity of the crystal chemistry of complex fluorides involving cations as Zr^{4+}, U^{4+}, Th^{4+}, and Ln^{3+}, which accept coordination numbers higher than 6 (7, 8, 9, or 11), is once more established.

REFERENCES

1. M. Poulain and B. C. Tofield, *J. Solid State Chem.* **39,** 314 (1981).
2. B. C. Tofield, M. Poulain, and J. Lucas, *J. Solid State Chem.* **27,** 163 (1979).
3. M. Poulain, M. Poulain, and J. Lucas, *Rev. Chim. Miner.* **12,** 9 (1975).
4. M. Poulain, M. Poulain, and J. Lucas, *J. Solid State Chem.* **8,** 132 (1973).
5. O. Graudejus, F. Schrötter, B. G. Müller, and R. Hoppe, *Z. Anorg. Allg. Chem.* **620,** 827 (1994).
6. J. P. Laval and A. Abaouz, *J. Solid State Chem.* **100,** 90 (1992).
7. P. P. Fedorov, M. D. Val'kovskii, O. S. Bondareva, and B. P. Sobolev, *Zh. Neorg. Khim.* **38**(10), 1611 (1993).
8. J. P. Laval and A. Abaouz, *J. Solid State Chem.* **96,** 324 (1992).
9. Yu. M. Korenev, P. I. Antipov, and A. V. Novoselova, *Zh. Neorg. Khim.* **25,** 1255 (1980).
10. A. I. Popov, M. D. Valkovskii, P. P. Fedorov, and Yu. M. Kiselev, *Zh. Neorg. Khim.* **36**(4), 842 (1991).
11. J. P. Laval, J. F. Gervais, L. Fournes, J. Grannec, P. Gravereau, A. Abaouz, and A. Yacoubi, *J. Solid State Chem.* **118,** 389 (1995).
12. E. Caignol, J. Metin, R. Chevalier, J. C. Cousseins, and D. Avignant, *Eur. J. Solid State Inorg. Chem.* **25,** 399 (1988).
13. J. C. Champarnaud-Mesjard, J. P. Laval, and B. Gaudreau, *Rev. Chim. Miner.* **11,** 735 (1974).

14. G. Fonteneau and J. Lucas, *J. Inorg. Nucl. Chem.* **36,** 1515 (1974).
15. J. F. Gervais, L. Fournes, J. Grannec, P. Gravereau, J. P. Laval, and P. Hagenmuller, *Mater. Res. Bull.* **29**(4), 405 (1994).
16. P. P. Fedorov, O. V. Pil'Gun, B. P. Sobolev, and P. I. Fedorov, *Zh. Neorg. Khim.* **35**(4), 1068 (1990).
17. M. N. Brechovski, A. I. Popov, Yu. M. Kiselev, A. L. Plinskii, and V. A. Fedorov, *Zh. Neorg. Khim.* **34**(4), 1021 (1989).
18. L. O. Gilpatrick and C. J. Barton, Reactor Chem. Div. Ann. Progr. Rept. for Period Ending May 31, ORNL-4717, 7 (1971).
19. J. Guery, Y. Gao, C. Guery, and C. Jacoboni, *Eur. J. Solid State Inorg. Chem.* **31,** 187 (1994).
20. G. M. Sheldrick, *Acta Crystallogr. A* **46,** 467 (1990).
21. M. O'Keeffe and B. G. Hyde, *Philos. Trans. R. Soc. London A* **295,** 553 (1980).